RESEARCHERID
THOMSON REUTERS

[Romero et al., 7(1): January, 2020] ISSN 2349-4506
Impact Factor: 3.799

Global Journal of Engineering Science and Research Management

THE ROLE THE PURITY OF CHEMICAL REAGENTS HAS ON THE CHEMICAL AND STRUCTURAL PROPERTIES OF GRAPHITE OXIDE AND THERMALLY REDUCED GRAPHENE OXIDE

A. Romero[1], J.L. Valverde[1], L. Sanchez-Silva[1] M.P. Lavin-Lopez[2], A. Patón-Carrero[1]
[1]University of Castilla-La Mancha, Department of Chemical Engineering, Avenida Camilo Jose Cela 12, 13071, Ciudad Real (Spain).
[2]Graphenano S.L., Calle Pablo Casals 13, 30510, Yecla, Murcia (Spain)

DOI: 10.5281/zenodo.3625621

KEYWORDS: graphite oxide; chemical reagents; Hummers method; graphene

ABSTRACT

A study into how the purity of the chemical reagents (H_2SO_4 and $KMnO_4$) influenced the chemical and structural properties of graphite oxide and graphene oxide reduced by low temperature, was carried out in order to develop low cost and viable industrial processes for the large-scale production of graphene-based materials. The samples were analyzed and explained on the basis of the following characterization techniques: Raman spectroscopy, SEM, TEM, FTIR, elemental analysis (EDX), X-ray diffraction, TGA, and, particle size analyzer. Data about the features of the graphene-based materials enable it to be determined whether, high purity chemicals normally supplied in low quantities at a high price, are or not needed in certain applications for the final graphene-based materials. In other words, in this paper how the impurities present in chemical reagents could influence the characteristics of the final products is analyzed).

INTRODUCTION

Graphene-based materials are a broad family of graphene nanomaterials containing graphene layers including multi-layer materials with few layers, graphite or graphite oxide materials and, modified forms of graphene oxide and reduced graphene oxide [1].

Graphite oxide (GrO) has received a great deal of attention for several years due to its exceptional properties such as its hydrophilic character, the functional groups found in it and, because it is considered to be an alternative to graphene and a platform of different composites for a range of applications [2]. GrO is prepared by the common Hummers method and variations of this [3], in which several chemical reagents are used. The resulting GrO must be exfoliated later on and reduced in order to obtain reduced graphene oxide. Exfoliation and GrO reduction, are vital processes because they will affect the production of reduced graphene oxide. Through thermal treatment, it is possible to simultaneously exfoliate and reduce the GrO. Moreover, the thermal process is more environmentally friendly than that based on the use of chemical reagents for reducing oxidized GrO and, in many cases, it can be more efficient [4]. In this respect, it is highly important to develop a thermal reduction method that does not involve using high temperatures (which have proven to be the most efficient).

Apart from this, one of the main scientific, engineering and financial challenges that needs to be faced today is large-scale production of GrO. To date, Hummers is the best method for producing large quantities of GrO (easily scalable for industrial production). An important challenge in the synthesis of large-scale GrO , is supplying large quantities of starting materials (mainly raw graphite and chemical reagents such as $KMnO_4$ and H_2SO_4) suitable for the cost-effective production of GO. Among these chemical reagents, sulfuric acid is used as an intercalating agent and potassium permanganate as the oxidant agent which is conducive to oxidation. Fortunately, the H_2SO_4 intercalating chemical is readily available on an industrial scale as it is one of the most heavily traded chemicals in the world [5]. Nevertheless, from an industrial perspective, using potassium permanganate can be dangerous if proper precautions are not taken and, it is an expensive product. Since the Hummers process and variants of it typically use a $KMnO_4$/graphite= 3/1 mass ratio, it is logical to think that the oxidant is a very significant factor in the total operating costs [6]. Both chemical reagents, will influence the quality of the GrO produced. For many applications, the highest purity chemicals are not needed and, all that is required is a simple cost-effective solution of a reliable quality which is available in large quantities. However, sometimes chemical reagents supplied in

large quantities, although much cheaper, may contain impurities that could influence the characteristics of the final product.

In this paper, different graphite oxides (GrO) and thermally reduced graphene oxide (trGO) samples have been synthesized using a controlled process based on the chemical oxidation of bulk graphite powder (following a procedure on the basis of the Improved Hummers method), followed by thermal reduction at very low temperatures. In this research, oxidation was controlled by the purity of the chemical reagents used (H_2SO_4 and $KMnO_4$). All the synthesized samples underwent exhaustive characterization in order to find out what the most important details were which influenced how pure the chemical reagents were that were used in the synthesis on the morphological, structural and chemical aspects of the samples.

MATERIALS AND METHODS

Materials

The graphite powder and HCl (purity ≥ 37%) were supplied by Sigma-Aldrich, H_2O_2 (33% purity) and the ethanol (99.5% purity) was supplied by Panreac. $KMnO_4$ (97-99% purity) and the H_2SO_4 (96-98% purity) was provided by three different suppliers and used for synthesizing three different graphite oxides: GrO1, GrO2 and GrO3. According to the technical specifications of the different reagents (Table 1), all three sulfuric acids were similar in purity (97-98%) although, the metal (mainly Fe), chlorides and SO_2 content was much higher in the H_2SO_4 used for synthesizing GrO2 and GrO3. As regards $KMnO_4$, the chemical composition of the chemical products used for synthesizing GrO2 and GrO3, was similar in terms of chlorides, sulfates and, insoluble matter and considerably higher than those in the $KMnO_4$ used for synthesizing the GrO1 sample.

In summary, the chemical reagents used for synthesizing the GrO2 and GrO3 graphite oxide samples showed traces of impurities (maximum amounts in the ppm range) which were also present (albeit in a much smaller amount) in the reagents used for synthesizing the GrO1 sample. Note, the main impurities were present in more significant quantities in the three different oxidants ($KMnO_4$), but not so much in the acid medium (H_2SO_4).

Table 1. Chemical composition of the reagents used in oxidation

$KMnO_4$	**GrO1**	**GrO2**	**GrO3**
Assay (%)	> 99%	> 98	> 98%
Chlorides (max ppm)	100	1000	1000
Sulfates (max ppm)	300	2000	2000
Insoluble matter (max ppm)	200	10000	10000
H_2SO_4	**GrO1**	**GrO2**	**GrO3**
Assay (%)	98	98	98
Cl (max ppm)	0.1	10	4
SO_2 (max ppm)	2	15	20
Fe (max ppm)	0.1	15	20
Other Metals (ppm)	10	9	9

Synthesis of Graphite Oxide (GrO) and Thermally Reduced graphene oxide (trGO)

Graphite oxide was synthesized following the Improved Hummers Method with some modifications [7]. A mixture of 15 grams of graphite and 45 grams of $KMnO_4$ (oxidizer agent) was slowly added in a 400ml solution of H_2SO_4 under constant agitation and this was maintained at 50ºC for 3 hours. Then, in order to stop the oxidation reaction, the mixture was poured into a beaker containing a mixture of 400 g of flake ice and 3ml of H_2O_2. This mixture underwent vacuum filtration and finally, it was washed with 200 ml of deionized water, HCl and CH_3CH_2OH. Finally, the compact cake was dried at 100 ºC overnight and the samples were named GrO.

Thermal reduction was carried out by placing graphite oxide in a laboratory drying oven at low temperatures (<300ºC). The material expanded after a certain time, with the graphene layers separating and, some oxygen-containing functional groups were removed from the structure. The products obtained were named trGO.

ISSN 2349-4506
Impact Factor: 3.799
Global Journal of Engineering Science and Research Management

Characterization techniques

The Fourier transform infrared (FTIR) spectra analysis was carried out with a SPECTRUM TWO spectrometer (Perkin Elmer, Inc) and performed in transmission mode using KBr (350-8300 cm^{-1}) pellets and, ZnSe (550-6000 cm^{-1}). Raman spectra were obtained with a SENTERRA spectrometer using a 532nm excitation wavelength. Thermogravimetric analysis (TGA) data were recorded on a METTLER TOLEDO TGA/DSC1 instrument at a heating rate of 10 °C min^{-1} in air. Sample morphology was observed with a scanning electron microscopy (SEM) (Phenom ProX). The SEM was coupled to a microanalysis system and measured by means of energy dispersive X-ray spectroscopy (EDS) in order to obtain an elemental analysis of the powders. Transmission electron microscopy (TEM) images were obtained with a JEOL JEM 1400 electronic microscope. Particle size was measured by using a Mastersizer 2000 Hydro module. The powder X-ray diffraction (XRD) analysis was carried out with a diffractometer (PHILIPS, PW-1711) with CuKα radiation (λ = 1.5404 Å). The crystallographic parameters (interlaminar space (d); crystal stack height (Lc); in-plane crystallite size or layer size (La) and, number of graphene layers in the crystal (Nc) were determined as follows [8, 9]:

$$d = \frac{\lambda}{2 \cdot sen\theta_1} \; ; \quad L_c = \frac{k_1 \cdot \lambda}{FWHM \cdot cos\theta_1} \; ; \; L_A(nm) = \frac{k_2 \cdot \lambda}{FWHM \cdot cos\theta_2}$$

Where:

- λ, radiation wavelength (λ = 0,15404 nm)
- θ_1, [002] or [001] diffraction peak position (º)
- θ_2, [100] diffraction peak position (º)
- k_1, Form factor (k=0,9)
- k_2, Warren Form Factor constant (k=1,84)
- $FWHM$, Width at half the height of the corresponding diffraction peak (rad)

RESULTS AND DISCUSSION

Table 2 shows an elemental analysis of the composition (mainly C and O content) of the different graphene-based materials. The results indicated that, after oxidation to graphite oxide, over 40% of the oxygen atoms were always introduced into the carbon structure of graphite by way of oxygen-containing functional groups. Note that, the residual Cl content was significantly higher in samples GrO2 (9%) and GrO3 (4%) compared to that in GrO1 (1%). This was directly related to the higher Cl content, mainly in the H2SO4 there was in the GrO2 synthesis but also, to the higher amount of chlorines in the KMnO4. After thermal reduction, the oxygen-containing functional groups were reduced to around 35wt% in GrO1 and 26wt% and 27 wt% in the GrO2 and GrO3 samples, respectively. The C/O ratio was kept constant (1.1) for the oxidized samples while the C/O ratio for the reduced samples showed higher values (2.2) for the more reduced sample and which, consequently, contained a smaller percentage of oxygen groups (trGO3). This C/O rate value fell when the percentage of oxygen rose and values of 2.8 and 1.8 were obtained for the trGO2 and the trGO3, respectively.

ISSN 2349-4506
Impact Factor: 3.799
Global Journal of Engineering Science and Research Management

Table 2: Characterization parameters of the GrO and trGO samples.

	Elemental analysis				XRD crystallographic parameters					Particle size		
Sample	**C (%)**	**O (%)**	**Cl (%)**	**Ratio C/O**	**d (nm)**	**FWHM (º)**	**L_C (nm)**	**L_A (nm)**	**npg**	**D_{10} (µ)**	**D_{50} (µ)**	**D_{90} (µ)**
GrO1	51	48	1	1.1	0.89	1.4	4.38	9.73	5	10.4	30.8	62.6
trGO1	65	35	-	1.8	0.38	3.7	2.18	8.32	6	5.5	15.3	35.1
GrO2	48	43	9	1.1	0.98	1.6	4.74	10.37	5	4.2	12.5	24.1
trGO2	74	26	-	2.8	0.37	6.4	1.26	5.96	5	8.6	23.4	50.8
GrO3	51	45	4	1.1	0.85	2.2	3.56	7.33	5	5.0	17.1	39.2
trGO3	68	27	1	2.2	0.37	5.3	1.87	6.24	4	5.6	17.9	45.5

FWHM: Full width at half-maximum corresponding to [002] peak for trGO or [001] peak for GrO samples.
d: interlayer distance
L_c, L_A: mean crystallite diameters
npg: average number of sheets in crystallite (L_c/d).
D_{10}, D_{50} and, D_{90}: particles sizes at which 10%, 50% and, 90% of the sample is below this given size.

Raman spectra of the GrO samples (Figure 1a) showed the D and G bands to be located at 1345 and 1575 cm_{-1} respectively [10]. The D band has been attributed to defects or to the breakdown of translational symmetry in the graphite lattice [11]. In turn, the G band corresponded to the Brillouin zone (BZ) of the crystal line sp^2 lattice in graphite. The integrated intensity ratio I_D/I_G for the D and G bands is a widely used parameter for characterizing the quantity of defects in graphitic materials [12]. The results obtained clearly showed that, after oxidation (regardless of how pure the chemical reagents were), the high I_D/I_G ratio (compared to that of the raw graphite, (≈0.11) indicated there was a high number of defects and a low degree of graphitization. The I_D/I_G ratios were quite similar in the three samples (the small differences observed could not be clearly explained by how pure the chemical reagents were) [13]. Moreover, the distance between the defects was estimated (determined as $L_D = \sqrt{(C(\lambda)/(ID/IG))}$ being $C(\lambda)=102$ nm^2) and almost no differences between the samples were found.

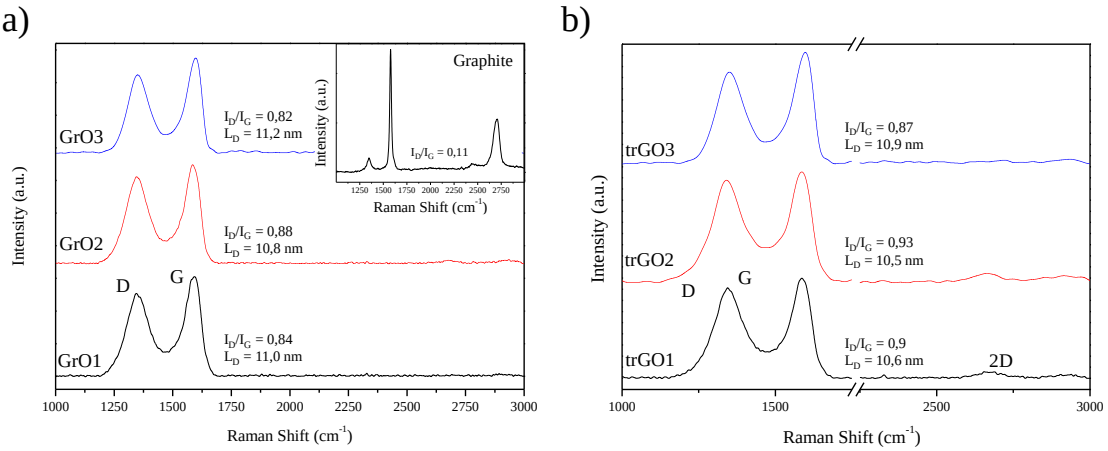

Figure 1. Raman spectra of a) graphite oxide samples, b) thermal reduced graphite oxide samples.

The FTIR spectroscopy (Figure 2a) revealed differences in the functional groups between the different oxidized samples. Several functional groups were incorporated into the graphitic structure after oxidation [14]: a sharp peak, explained by the O-H stretching vibrations of a hydroxyl group and water molecules, appears in the 3100-3600 cm^{-1} range. Moreover, the deformation vibration modes of the C-OH groups at around 1430 cm^{-1} can be seen.

The bands located at around 3010 and 2950 cm^{-1} corresponding to the stretching vibrations of alkene groups (C-H) and CH_2/CH_3 respectively, were clearly visible in the GrO2 sample. Note, these bands may have been related to ethanol residues from the sample washing phase. The stretching vibrations of CH_2/CH_3 could also be observed at low wavelength values of 850 cm^{-1}. In turn, the band located at approximately 1630 cm^{-1} which was attributed to the C=C skeletal vibration of the graphene planes, was clearly visible in all samples, indicating the graphene structural integrity after oxidation was stable.

Furthermore, the band appearing at around 1750 cm^{-1}, attributed to the C=O stretching vibration of a carbonyl group, was clearly visible in all samples. The peak at 1220-1230 cm^{-1}, which represented the stretching vibration of the epoxy C-O-C group, was clearly a sharp one only in sample GrO1. A broad band at around 1050-1100 cm^{-1} which was attributed to the C-O stretching vibration of an alkoxy group, could be seen in all samples but, it was more prominent in samples GrO2 and GrO3 [10, 13, 14].

Finally, the sharp peak at around 1250 cm^{-1} due to the C-H wag in terminal alkyl halides ($-CH_2Cl$),could be dimly seen in the GrO2 and GrO3 samples which is in keeping with the elemental analysis results, where the remains of Cl were visible in these samples (mainly in GrO2). The alkyl chlorine compound could also be observed at a vibration frequency of around 760 cm^{-1} (C-Cl stretch).

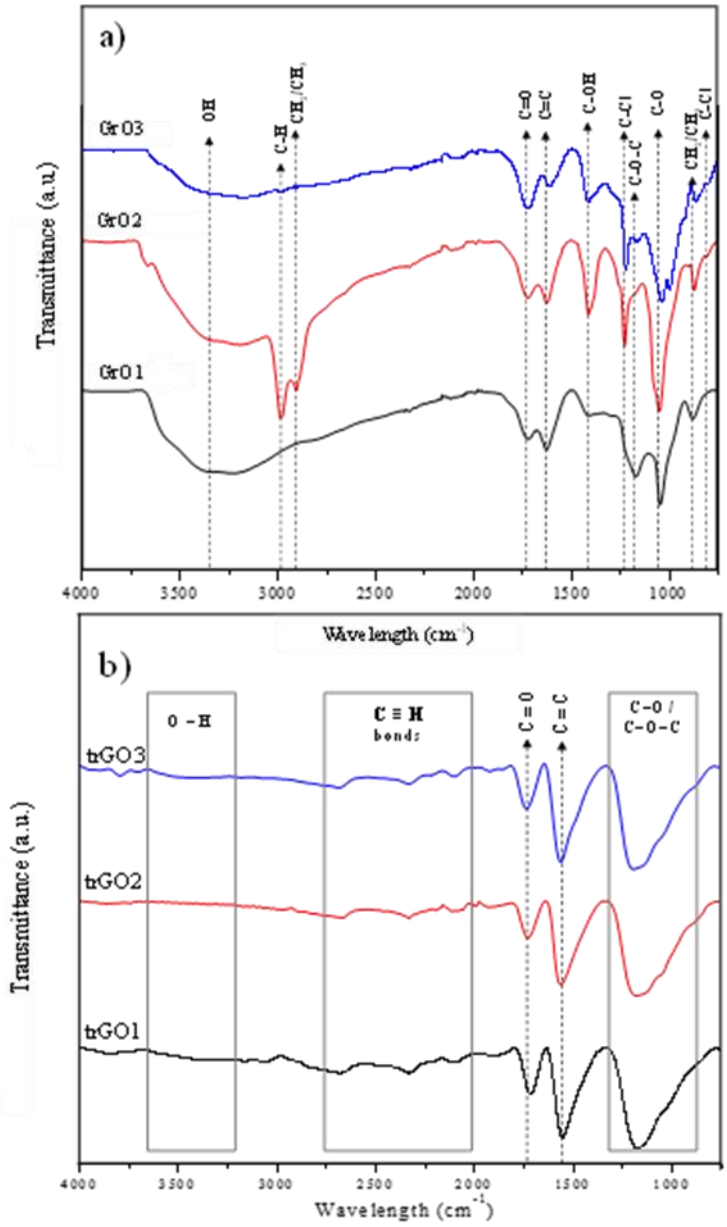

Figure 2. FTIR spectra of a) graphite oxide samples, b) thermal reduced graphite oxide samples.

According to the FTIR results, all evidence seems to indicate that, the attack on the graphite structure that takes place during oxidation, was different depending on how pure the chemical reagents used during the oxidative treatment were. The FTIR results suggest the chemical reagents used in the synthesis of the GrO2 and GrO3 samples were not conducive to attacks on the graphite structure network with epoxy groups, which could be explained by the greater amount of impurities in the $KMnO_4$ used in their synthesis. In other words, the chemical reagents used for synthesizing the GrO1 sample, harshly attacked the graphite structure, introducing both hydroxyl and epoxy groups into it, while there were carbonyl and alkoxy groups in all samples. According to several

authors, epoxy and alkoxy functionalities attack the basal plane while, hydroxyl functional units and carbonyl groups are mainly located at the edges of the planes of graphene layers [11, 15].

The XRD patterns and parameters of the oxidized samples are shown in Figure 3a and Table 1, respectively. As can be seen, all the oxidized samples showed the typical diffraction peaking which is characteristic of graphite oxide ((001) peak) at around 10° while the peak at 26.6° (ascribed to the (002) face of graphite and corresponding to an inter-layer distance of 0.34 nm) disappeared because of oxidation. It must be stressed that, the (001) peak position was slightly lower in the GrO2 sample than in the other ones, thus showing the highest basal spacing (0.98 nm) in comparison with the GrO1 and GrO3 samples, which had values of 0.89 and 0.85 nm, respectively. The (001) wide (FWHM values), relating to the crystallite sizes, had an inverse relationship with both the LA and Lc values [16]. The height of the crystallites (Lc) was seen to decrease after oxidation from 37nm in the bulk graphite (not shown) to around 4.7-3.6nm in the oxidized samples. In turn, the size of the crystallite layer (LA) was determined to be in the 7.3-10.3 nm range [8].
The XRD results must be explained by taking the FTIR and elemental analysis findings into account. Thus, in GrO2, with a high amount of oxygen groups (hydroxyls groups) edge-functionalized graphene planes and a minimal amount of epoxy groups, the hydroxyl-hydroxyl interactions which mainly take place at the edges of the graphene sheets does not help the graphite oxide sheets to couple, which causes the highest basal spacing. However, in the GrO1 sample, where there is a dense epoxy network and also, a large amount of hydroxyl groups linked at the edges, epoxy-hydroxyls interactions (hydrogen bonding between the basal plane and the edges of the sheets) would make it easier for the graphite oxide sheets to couple, which would cause a lower basal spacing compared to that in the GrO2 sample. Finally, the apparently smaller number of hydroxyls groups there were , , in the GrO3 sample, according to the FTIR results, with the remaining oxygen functionalities still present (mainly the carbonyl and alkoxy groups) except the epoxy ones, caused the lowest basal spacing.

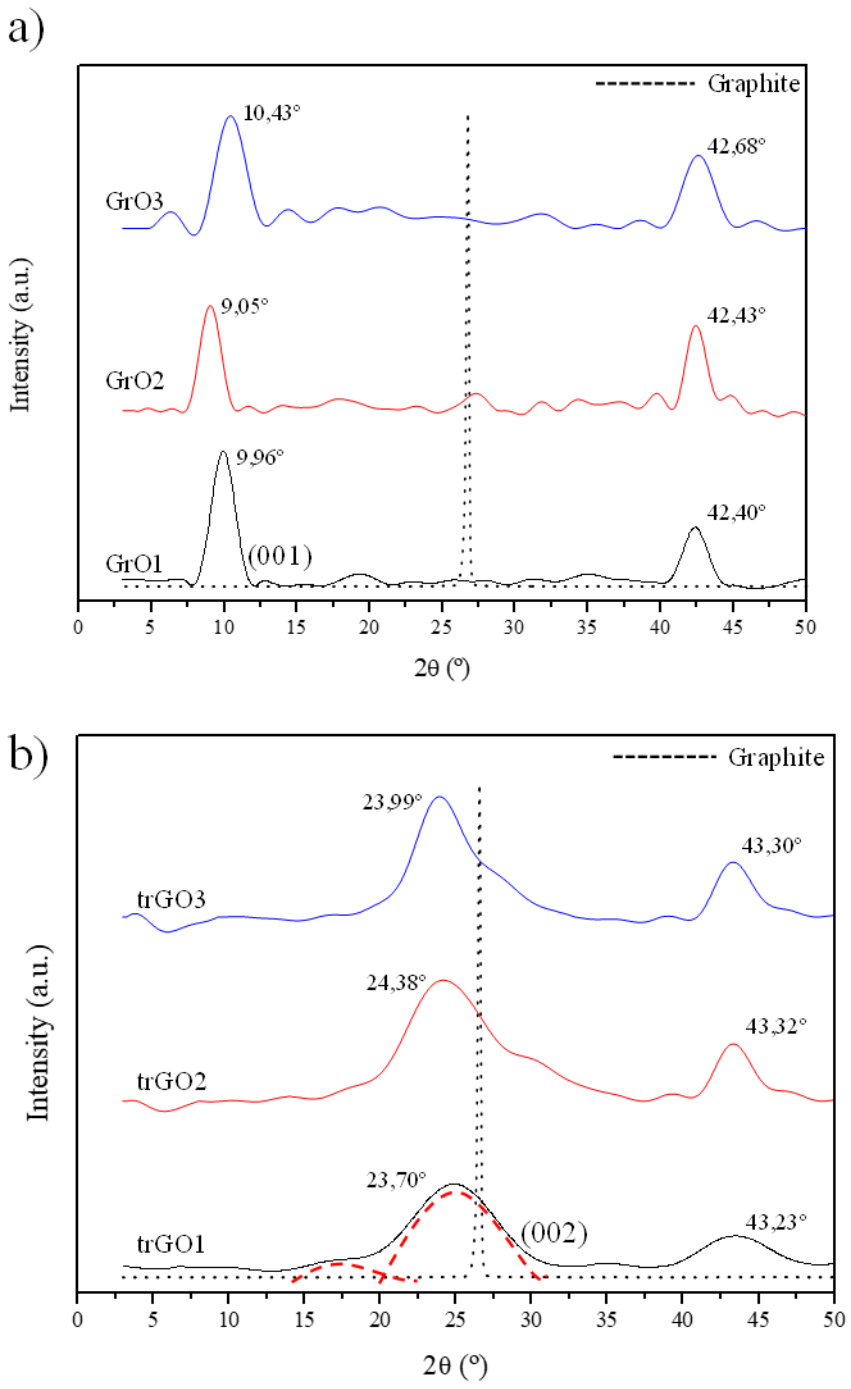

Figure 3. XRD spectra of a) graphite oxide samples, b) thermally reduced graphite oxide samples.

The OH functional groups were mainly reduced during thermal reduction at low temperature, which was confirmed by the FTIR results (Figure 2b). It was demonstrated that, the broad band corresponding to the hydroxyl groups (centered around 3400 cm^{-1}) disappeared, thereby bringing about different hydrogen bond rearrangements. In addition, the FTIR bands associated with the C–H alkene and CH_2/CH_3 groups in GrO2, also disappeared after reduction which could be indicative of a decrease in the sp^3 domains. Nevertheless, thermal reduction was not conducive to removing the carbonyl groups, which may even have increased in the reduced samples. It can be assumed that, the presence of air whilst the GrO was undergoing thermal treatment led to the formation of some new oxygen groups or the transformation of non-carboxyl functionalities into these groups [17]. The peak attributed to the aromatic C=C group appeared to be very sharp, indicating that prominent sp^2 graphitic domains were constantly generated and, displaced to lower wavenumbers in thermally reduced samples, which has been explained by a stronger hydrogen bond coordination between the oxidized graphene sheets [15]. Moreover, a broad band appearing between 800 and 1300 cm^{-1}, was attributed to the overlapping C-O and C-O-C (when present) groups, indicating that those groups were not removed (or poorly removed) after thermal reduction.

The XRD results confirmed functional groups and oxygen and hydrogen moisture were partially removed. This reaction was followed by a rapid removal of gaseous products so that, the initial stacked structure was partially restored in the trGO samples, with the diffraction peak appearing again (002) but displaced to values in the low twenties (around 24° instead of 26.6º appearing in graphite). This broad (002) peak in the trGO samples, would correspond to the non-crystalline stacks of graphene layers in the particles (few graphene layers) [11]. The shoulder at around 16-17° which clearly appears in the trGO1 sample, corresponds to the remaining oxygen-containing groups. As can be seen, the crystal domains (L_C and L_A) decreased after thermal reduction due to the rise in structural disorder. This finding was also corroborated by the diffraction peak which appeared at around $2\theta = 42.5°$ in the XRD pattern of the GrO samples, which has been linked to turbostratic disorder [18, 19] and that broadened and shifted at higher 2θ values after thermal reduction, indicating an increase in structural disorder.

The XRD results were corroborated by the RAMAN spectroscopy analyses (Figure 1b). After thermal reduction, the I_D/I_G ratio slightly increased compared to that for the oxidized samples, indicating that during reduction, the GrO structure was altered and the structural defects were seen to persist and even increase despite partially removing the oxygen-containing functional groups [20]. Moreover, the 2D band (ascribed to the second order double resonant Raman scattering from zone boundary) becomes visible at around 2700 cm^{-1}, confirming the rearrangement of the carbon lattice after thermal reduction.

Research into the thermal stability of synthesized GrO and trGO was performed using Thermal Gravimetric Analysis (TGA), with the results shown in Figure 4. Four different weight loss steps could be differentiated in the GrO thermographs. In the first one, at temperatures below 150 ºC, a weight loss in the range 14-17% was observed, due to the removal of water solvent molecules (both physisorbed and interlamellar) although, unstable functional groups also started degrading. The second weight loss step, occurring between 150 and 200ºC approximately, was the thermally induced decomposition of the more labile oxygen functional groups and subsequent release of steam and gases (CO, CO2). A weight loss of 22, 18 and, 16% was observed for GrO1, GrO2 and GrO3, respectively. In the third step, which occurred between 200 and 450ºC approximately, the more thermally stable oxygen groups were removed and a weight loss of 22, 14 and, 23% was observed for GrO1, GrO2 and GrO3, respectively [21]. Finally, there was a fourth weight loss step at temperatures above 450ºC, as a consequence of thermal degradation of the material, which lost around 38-42% of its remaining mass.

Moreover, a TGA of the reduced samples was also carried out in order to analyze what oxygen groups remained after heat treatment. Important differences could be observed after thermally reducing the samples. In all cases, the weight loss corresponding to the removal of the different functional groups in the reduction samples was much lower in comparison to that of the oxidized samples. However, with the sample trGO1, the same weight loss steps presented in GrO1 could be seen, and the carbonaceous structure began degrading at around 450 ºC, a temperature similar to that observed in the corresponding GrO1. However, thermal reduction for the GrO2 and GrO3 samples resulted in a much more abrupt expansion, which was conducive to removing the functional groups anchored to the graphene layers. As can be seen, the weight loss at temperatures below 400 °C, was 26, 10 and 12% for samples trGO1, trGO2 and trGO3, respectively. These differences in weight loss, indicate that, the oxygen functionalities present in the GrO2 and GrO3 samples were reduced more easily during thermal reduction. Thus, the remaining functional groups in trGO2 and trGO3 mainly decomposed at temperatures above 400 ºC with continuous weight loss overlapping with that corresponding to the thermal degradation of the carbonaceous

structure. In other words, the greater thermal stability up to 400 ºC observed in samples trGO2 and trGO3, has been explained by the higher degree of de-oxygenation in them. As observed, at temperatures above 400 ºC, the thermal stability of the trGO2 and trGO3 samples dropped abruptly with a weight loss much higher than that observed for trGO1.

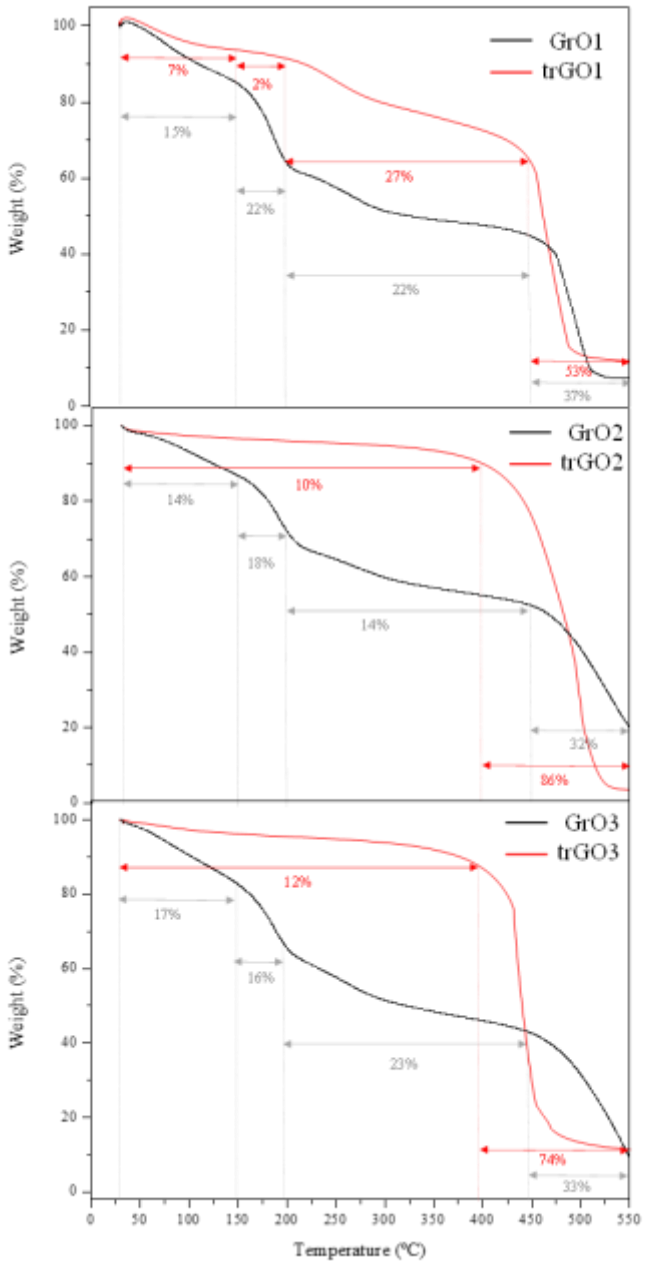

Figure 4. TGA spectra of graphite oxide and thermally reduced graphite oxide samples.

A quantitative evaluation of dispersion particle size (the particle size of the dried samples dispersed in water) is shown in Table 1. It must be stressed that, in comparison with the particle size of the raw graphite (D90 = 45 μm), oxidation gave rise to an increase in particle size in the GrO1 sample and, on the contrary, a decrease in the GrO2 and GrO3 samples. Conversely, after thermal reduction, there was a considerable increase in particle size in samples trGO2 and trGO3 (denser packing of particles) due to the high amount of oxygen-containing functional groups removed from them, as commented on above.

The morphology of the synthesized graphene materials can be seen in the TEM images shown in Figure 5. Intercalation of solvated $SO4^{2-}$ molecules, which opened the defective sites at the edges and even entered into the intervening space through oxidation, weakened the van der Waals forces between the graphene layers, which resulted in the graphite transforming into GrO, with a significant deformation in the raw graphite structure (not shown). Thus, as can be seen in the GrO images, there was a clear delamination in the carbon material after oxidative treatment with the graphene layers creasing. This high level of corrugation has, on previous occasions, been connected to localized intrinsic strain due to oxygen-containing functional groups loading on the graphene sheets [15]. After heat shock treatment for the GrO samples, the graphene layers were damaged, twisting and crumbling due to the abrupt release of gaseous products such as CO and CO_2 which disordered the graphitic structure whilst the graphene layers were partially separating [17]. In any event, the layered structure was partially preserved after deep oxidation and subsequent thermal reduction.

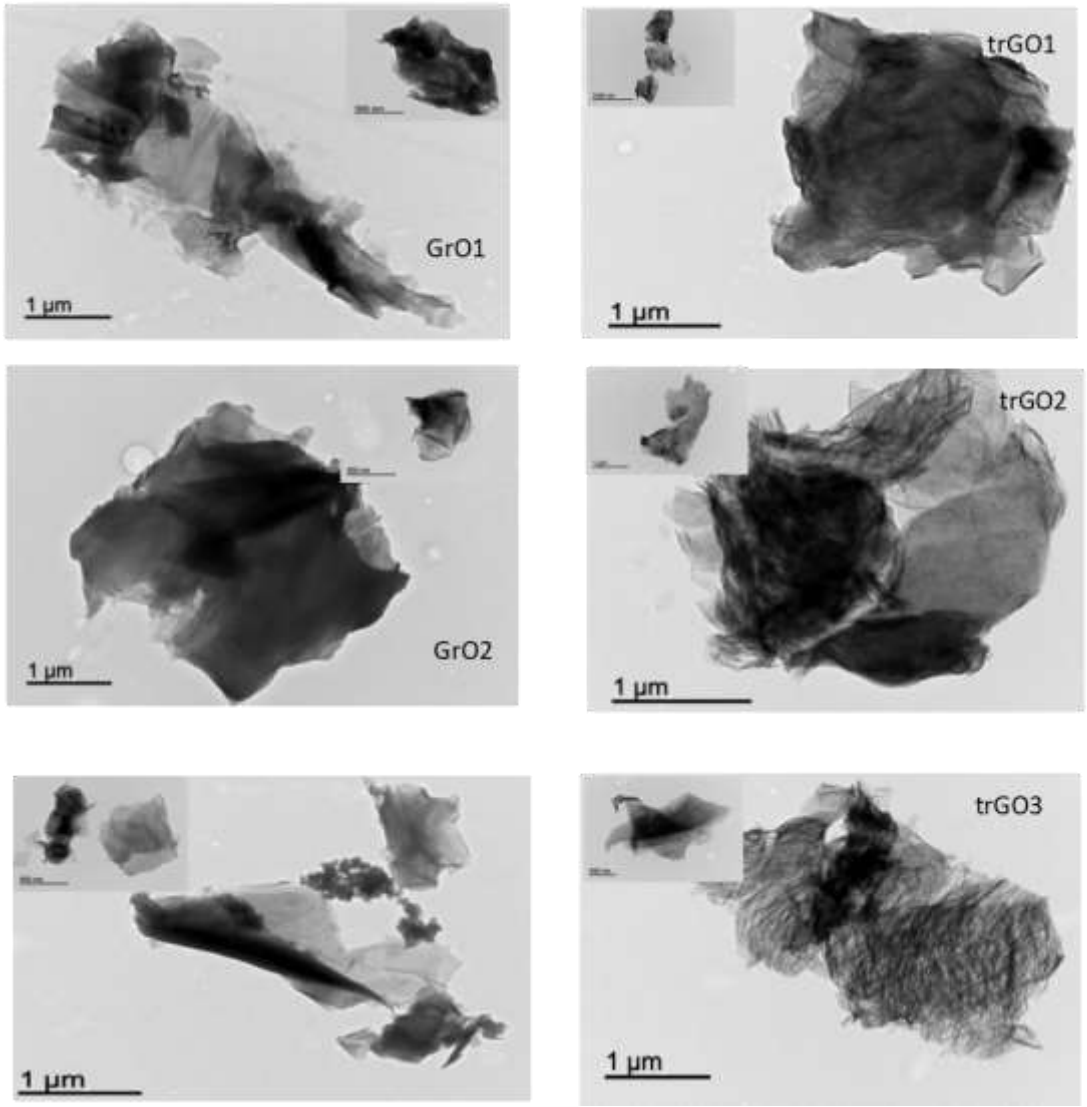

Figure 5. TEM micrographs for the GrO and trGO samples

The influence of the purity of the chemical reagents (H_2SO_4 and $KMnO_4$) on the chemical and structural properties of graphite oxide and graphene oxide reduced by low temperature, was studied in order to develop low cost and viable industrial processes for producing graphene-based materials. Graphite oxides with a high degree of oxidation were obtained regardless of how pure the reagents were, The purity of the reactants (mainly focused on the $KMnO_4$ purity) was shown to influence the type of oxygen-containing functional groups introduced during oxidation. So the harsher oxidizing conditions obtained with the highest purity reagents (GrO1 sample), were favorable to the introduction of a large quantity of oxygen-containing functional groups, many of which were epoxides as well as hydroxyls, carbonyl and alkoxy groups. Furthermore, the oxygen groups in the structure of the samples synthesized using the KMnO4 with most impurities (the GrO2 and GrO3 samples), characterized by the low presence of epoxy groups, were more easily removed by low temperature reduction, and expansion was far more abrupt throughout this thermal process.
Finally, theoretical and experimental studies have revealed that fine-tuning the chemical composition, the crystallinity or the thermal properties of both GrO and trGO could be essential to the end uses of these graphene-related materials [22] such as for, sensors [23, 24] , lubricant additives [11] , capacitors and supercapacitors [2, 25], composite or biomedical materials [26].

CONCLUSION

The influence of the purity of the chemical reagents (H_2SO_4 and $KMnO_4$) on the chemical and structural properties of graphite oxide and graphene oxide reduced by low temperature, was studied in order to develop low cost and viable industrial processes for producing graphene-based materials. Graphite oxides with a high degree of oxidation were obtained regardless of how pure the reagents were. The purity of the reactants (mainly focused on the $KMnO_4$ purity) was shown to influence the type of oxygen-containing functional groups introduced during oxidation. so, the harsher oxidizing conditions obtained with the highest purity reagents (GrO1 sample), were favorable to the introduction of a large quantity of oxygen-containing functional groups, many of which were epoxides as well as hydroxyls, carbonyl and alkoxy groups. Furthermore, the oxygen groups in the structure of the samples synthesized using the $KMnO_4$ with most impurities (the GrO2 and GrO3 samples), characterized by the low presence of epoxy groups, were more easily removed by low temperature reduction, and expansion was far more abrupt throughout this thermal process.
Finally, theoretical and experimental studies have revealed that fine-tuning the chemical composition, the crystallinity or the thermal properties of both GrO and trGO could be essential to the end uses of these graphene-related materials [22] such as for, sensors [23, 24] , lubricant additives [11] , capacitors and supercapacitors [2, 25], composite or biomedical materials [26].

ACKNOWLEDGEMENTS

The authors acknowledge financial support from the Spanish company Graphenano Nanotechnologies UCTR16017

REFERENCES

1. Bianco, A., H.-M. Cheng, T. Enoki, Y. Gogotsi, R.H. Hurt, N. Koratkar, T. Kyotani, M. Monthioux, C.R. Park, J.M.D. Tascon and J. Zhang, "All in the graphene family – A recommended nomenclature for two-dimensional carbon materials" in CARBON vol. 65, 2013, pp. 1-6.
2. Tran, M.-H. and H.K. Jeong, "Economical Thermal Reduction of Graphite Oxide for Supercapacitor Applications" in NEW PHYSICS: SAE MULLI vol. 67, 2017, pp. 333-337.
3. Sarkar, G., N.R. Saha, I. Roy, A. Bhattacharyya, A. Adhikari, D. Rana, M. Bhowmik, M. Bose, R. Mishra and D. Chattopadhyay, "Cross-linked methyl cellulose/graphene oxide rate controlling membranes for in vitro and ex vivo permeation studies of diltiazem hydrochloride" in RSC ADVANCES vol. 6, 2016, pp. 36136-36145.
4. Tran, M.-H. and H.K. Jeong, "Effective reduction of graphene oxide for energy-storage devices" in NEW PHYS vol. 65, 2015, pp. 240-244.

5. Lowe, S.E. and Y.L. Zhong, Challenges of Industrial-Scale Graphene Oxide Production, in Graphene Oxide, A.M. Dimiev and S. Eigler, Editors. 2016.
6. Zhu, Y., D.K. James and J.M. Tour, "New routes to graphene, graphene oxide and their related applications" in ADVANCED MATERIALS vol. 24, 2012, pp. 4924-4955.
7. Lavin-Lopez, M.d.P., A. Romero, J. Garrido, L. Sanchez-Silva and J.L. Valverde, "Influence of Different Improved Hummers Method Modifications on the Characteristics of Graphite Oxide in Order to Make a More Easily Scalable Method" in INDUSTRIAL AND ENGINEERING CHEMISTRY RESEARCH vol. 55, 2016, pp. 12836-12847.
8. Stobinski, L., B. Lesiak, A. Malolepszy, M. Mazurkiewicz, B. Mierzwa, J. Zemek, P. Jiricek and I. Bieloshapka, "Graphene oxide and reduced graphene oxide studied by the XRD, TEM and electron spectroscopy methods" in JOURNAL OF ELECTRON SPECTROSCOPY AND RELATED PHENOMENA vol. 195, 2014, pp. 145-154.
9. Warren, B., "X-ray diffraction in random layer lattices" in PHYSICAL REVIEW vol. 59, 1941, pp. 693.
10. Romero, A., M. Lavin-Lopez, L. Sanchez-Silva, J. Valverde and A. Paton-Carrero, "Comparative study of different scalable routes to synthesize graphene oxide and reduced graphene oxide" in MATERIALS CHEMISTRY AND PHYSICS vol. 203, 2018, pp. 284-292.
11. Gupta, B., N. Kumar, K. Panda, V. Kanan, S. Joshi and I. Visoly-Fisher, "Role of oxygen functional groups in reduced graphene oxide for lubrication" in SCIENTIFIC REPORTS vol. 7, 2017, pp. 45030.
12. Pimenta, M., G. Dresselhaus, M.S. Dresselhaus, L. Cancado, A. Jorio and R. Saito, "Studying disorder in graphite-based systems by Raman spectroscopy" in PHYSICAL CHEMISTRY CHEMICAL PHYSICS vol. 9, 2007, pp. 1276-1290.
13. Alazmi, A., S. Rasul, S.P. Patole and P.M. Costa, "Comparative study of synthesis and reduction methods for graphene oxide" in POLYHEDRON vol. 116, 2016, pp. 153-161.
14. Drewniak, S., R. Muzyka, A. Stolarczyk, T. Pustelny, M. Kotyczka-Morańska and M. Setkiewicz, "Studies of reduced graphene oxide and graphite oxide in the aspect of their possible application in gas sensors" in SENSORS vol. 16, 2016, pp. 103.
15. Dreyer, D.R., S. Park, C.W. Bielawski and R.S. Ruoff, "The chemistry of graphene oxide" in CHEMICAL SOCIETY REVIEWS vol. 39, 2010, pp. 228-240.
16. Saha, U., R. Jaiswal and T.H. Goswami, "A Facile Bulk Production of Processable Partially Reduced Graphene Oxide as Superior Supercapacitor Electrode Material" in ELECTROCHIMICA ACTA vol. 196, 2016, pp. 386-404.
17. Gurzęda, B., T. Buchwald, M. Nocuń, A. Bąkowicz and P. Krawczyk, "Graphene material preparation through thermal treatment of graphite oxide electrochemically synthesized in aqueous sulfuric acid" in RSC ADVANCES vol. 7, 2017, pp. 19904-19911.
18. Emiru, T.F. and D.W. Ayele, "Controlled synthesis, characterization and reduction of graphene oxide: A convenient method for large scale production" in EGYPTIAN JOURNAL OF BASIC AND APPLIED SCIENCES vol. 4, 2017, pp. 74-79.
19. Nethravathi, C., J.T. Rajamathi, N. Ravishankar, C. Shivakumara and M. Rajamathi, "Graphite oxide-intercalated anionic clay and its decomposition to graphene− inorganic material nanocomposites" in LANGMUIR vol. 24, 2008, pp. 8240-8244.
20. Wojtoniszak, M. and E. Mijowska, "Controlled oxidation of graphite to graphene oxide with novel oxidants in a bulk scale" in JOURNAL OF NANOPARTICLE RESEARCH vol. 14, 2012, pp. 1248.
21. Tegou, E., G. Pseiropoulos, M. Filippidou and S. Chatzandroulis, "Low-temperature thermal reduction of graphene oxide films in ambient atmosphere: Infra-red spectroscopic studies and gas sensing applications" in MICROELECTRONIC ENGINEERING vol. 159, 2016, pp. 146-150.
22. Morimoto, N., T. Kubo and Y. Nishina, "Tailoring the oxygen content of graphite and reduced graphene oxide for specific applications" in SCIENTIFIC REPORTS vol. 6, 2016, pp. 21715.

23. Minitha, C.R., V.S. Anithaa, V. Subramaniam and R.T. Rajendra Kumar, "Impact of Oxygen Functional Groups on Reduced Graphene Oxide-Based Sensors for Ammonia and Toluene Detection at Room Temperature" in ACS OMEGA vol. 3, 2018, pp. 4105-4112.
24. Kavinkumar, T., D. Sastikumar and S. Manivannan, "Effect of functional groups on dielectric, optical gas sensing properties of graphene oxide and reduced graphene oxide at room temperature" in RSC ADVANCES vol. 5, 2015, pp. 10816-10825.
25. Sohail, M., M. Saleem, S. Ullah, N. Saeed, A. Afridi, M. Khan and M. Arif, "Modified and improved Hummer's synthesis of graphene oxide for capacitors applications" in MODERN ELECTRONIC MATERIALS vol. 3, 2017, pp. 110-116.
26. Das, S., S. Singh, V. Singh, D. Joung, J.M. Dowding, D. Reid, J. Anderson, L. Zhai, S.I. Khondaker, W.T. Self and S. Seal, "Oxygenated Functional Group Density on Graphene Oxide: Its Effect on Cell Toxicity" in PARTICLE & PARTICLE SYSTEMS CHARACTERIZATION vol. 30, 2013, pp. 148-157.